A baseline for microplastic particle occurrence and distribution in Great Bay Estuary

Matthew LH. Cheng
Department of Biological Sciences, University of New Hampshire, 38 Academic Way, Durham, NH 03824   USA
Lok.Cheng@unh.edu
@MLCheng3

Thomas C. Lippmann
University of New Hampshire, Department of Earth Sciences, Jere Chase Ocean Engineering Lab, 24 Colovos Road, Durham, NH   03284   USA
T.Lippmann@unh.edu
@LippmannThomas

Jennifer A. Dijkstra
Center for Coastal and Ocean Mapping, Chase Ocean Engineering Lab, 24 Colovos Road, Durham, NH 03824   USA
Jennifer.Dijkstra@unh.edu
@DijkstraLab

Gabriela Bradt
University of New Hampshire Cooperative Extension, 59 College Road, Durham, NH   03824   USA
Gabriela.Bradt@unh.edu
@DrSquidgNH

Salme Cook
University of New Hampshire, Department of Earth Sciences, Jere Chase Ocean Engineering Lab, 24 Colovos Road, Durham, NH   03284   USA
salme.cook@gmail.com

Jang-Geun Choi
University of New Hampshire, Department of Earth Sciences, Jere Chase Ocean Engineering Lab, 24 Colovos Road, Durham, NH   03284   USA
jc1404@wildcats.unh.edu

Bonnie L. Brown
University of New Hampshire, Department of Biological Sciences, 38 Academic Way, Durham, NH 03824   USA
Bonnie.Brown@unh.edu
@B3EcoGenetics

Corresponding author: Bonnie.Brown@unh.edu, University of New Hampshire, Dept. of Biological Sciences, 38 Academic Way, Durham, NH 03824 USA

Abstract

We extracted and analyzed microplastics (MP) in archived sediment cores from Great Bay Estuary (GBE) in the Gulf of Maine region of North America. Results indicated that MP are distributed in GBE sediments, 0-30 cm, at an average occurrence of 116 ± 21 particles g^{-1} and that morphology varies by site and depth. Analysis by sediment depth and age class indicated that MP accumulation increased over several decades but recently (5-10 years) has likely begun to decrease. Hydrodynamic and particle transport modeling indicated that bed characteristics are a more controlling factor in MP distribution than typical MP properties and that the highest accumulation likely occurs in regions with weaker hydrodynamic flows and lower bed shear stress, e.g., eelgrass meadows and along fringes of the Bay. These results provide a baseline and predictive understanding of the occurrence, morphology, and sedimentation of MP in the estuary.

Keywords: microplastics, sedimentation, Great Bay Estuary

Plastics, in particular microplastics (MP: predominantly degraded plastic particles that are <5 mm), are the fastest growing pollutant in US coastal waters (Law, 2017). It is generally agreed that ~90% of MP that enter the water column eventually sink to the bottom (Kaiser et al. 2017) and that benthic sediments are a long-term sink for MP (vanCauwenberghe et al. 2015). As such, benthic communities are likely more susceptible to ingestion of MP. High prevalence of plastic ingestion (83%) in lobsters (*Nephrops norvegicus)* (Murray and Cowie 2011) and plastic loads in mussels (*Mytilus ediulis)* (34-178 particles/mussel) (Mathalon and Hill 2014) has previously been documented. As a result, increased exposure to plastics could potentially have negative physiological consequences in biota as demonstrated by reduced reproductive performance in oysters (*Crassostrea gigas;* Sussarellu et al. 2016). Our current understanding of accumulation of MPs over space and time and their natural temporal dispersion is limited (Arthur et al. 2009). Further, water treatment facilities have been upgraded and newly constructed facilities may capture and filter plastics better (Zhang et al. 2020). Spatial concentrations of MPs likely are affected by the presence of oyster reefs and eelgrass beds where structure and filter-feeding can trap or slow the transport of particles. Thus, establishing temporal and spatial baselines of ambient MP levels and predicted accumulation areas are necessary to determine whether MP concentrations have undergone temporal changes and to craft effective seafood cultivation strategies.

Although MP studies have increased exponentially over the past decade, many of these studies are concentrated in Europe and Australia, with fewer studies performed in North America (Granek et al. 2020). The focus of our study was to generate baseline data for the historical complement of MP in a hydrodynamically active estuary located in North America, and to enable broad-level modeling of particle distributions that will identify potential locations of high MP concentrations. To accomplish this, we recovered MP particles from preserved cores collected in 2016 at strategic locations in Great Bay Estuary (GBE), including sites that correspond to an ongoing EPA-NCCA program led by other investigators. Suspended MP particles were seeded in a numerical particle model (Choi et al. 2018) with velocity fields and bed shear stresses obtained from a verified hydrodynamic model of the GBE system (Cook et al. 2019; Cook et al. 2021) for determination of dispersion and distribution of MP accumulation at the seabed.

Great Bay Estuary (43°04'0.60"N, 70°52'4.19"W), located in coastal New Hampshire, is well-mixed as there are seven rivers that drain into it and strong currents that bring ocean water up into the heart of the Bay (Fig. 1). The strong currents of Piscataqua River along the Maine-New Hampshire border introduce oceanic water into the Bay and mix with numerous (typically) low-discharge rivers that provide freshwater sources (Short,1992). The estuary has established eelgrass meadows, though these beds are much reduced than beds observed in 2006 (Trowbridge 2007). The presence of eelgrass substantially affects the sedimentation processes in the estuary, and serves as a sink for suspended sediment and other particles (thus, very likely MPs). Elimination of eelgrass meadows due to eutrophication or other degradation processes exposes the stored sediment to bottom shear stresses that can re-suspend previously stored material (including any deposited MPs). Similarly, within GBE, there are only a few remaining

sites of natural oyster reefs that have survived environmental and anthropogenic changes over the past several decades. More than 20 oyster restoration projects involving a diversity of objectives, sizes, and methods have been completed in the state since 2000 (Konisky et al. 2012, 2014). Since the mid-2000s, the emphasis has been on full restoration-scale projects. Additional efforts are underway to determine the best way forward in developing additional oyster aquaculture sites to revitalize the oyster populations in the estuary and help local farmers. Unfortunately, whether these sites are sinks for MP is not known.

Pollution has become an issue forcing change, particularly from permitted waste-water treatment facilities (Mason et al. 2016; Murphy et al. 2016) located in 42 communities in New Hampshire and 10 communities in Maine. These facilities discharge directly into the seven tributaries of GBE and previous studies have found that these facilities discharge micro- and nano-plastics (particles ≤100 μm) as previous studies found these facilities to be important contributors to microplastic concentrations (Estahbanati and Fahrenfeld 2016, Mason et al. 2016, Murphy et al. 2016). Because the flow of water within GBE is complex and river input varies both spatially and temporally (Short, 1992), the extent to which rivers are the primary source of MPs is unclear. We also have no knowledge of where MPs concentrate once they are introduced. If particles concentrate at certain times of the year or in some areas but not others (e.g., wetlands, mud flats, oyster reefs, eelgrass beds, deep channels), better knowledge of the dispersal and settling of MP would provide harvesters, aquaculturists, and resource managers with the necessary information to evaluate contaminant risks, choose low MP sites for their activities, and provide information on the time of year with the highest or lowest MP concentrations.
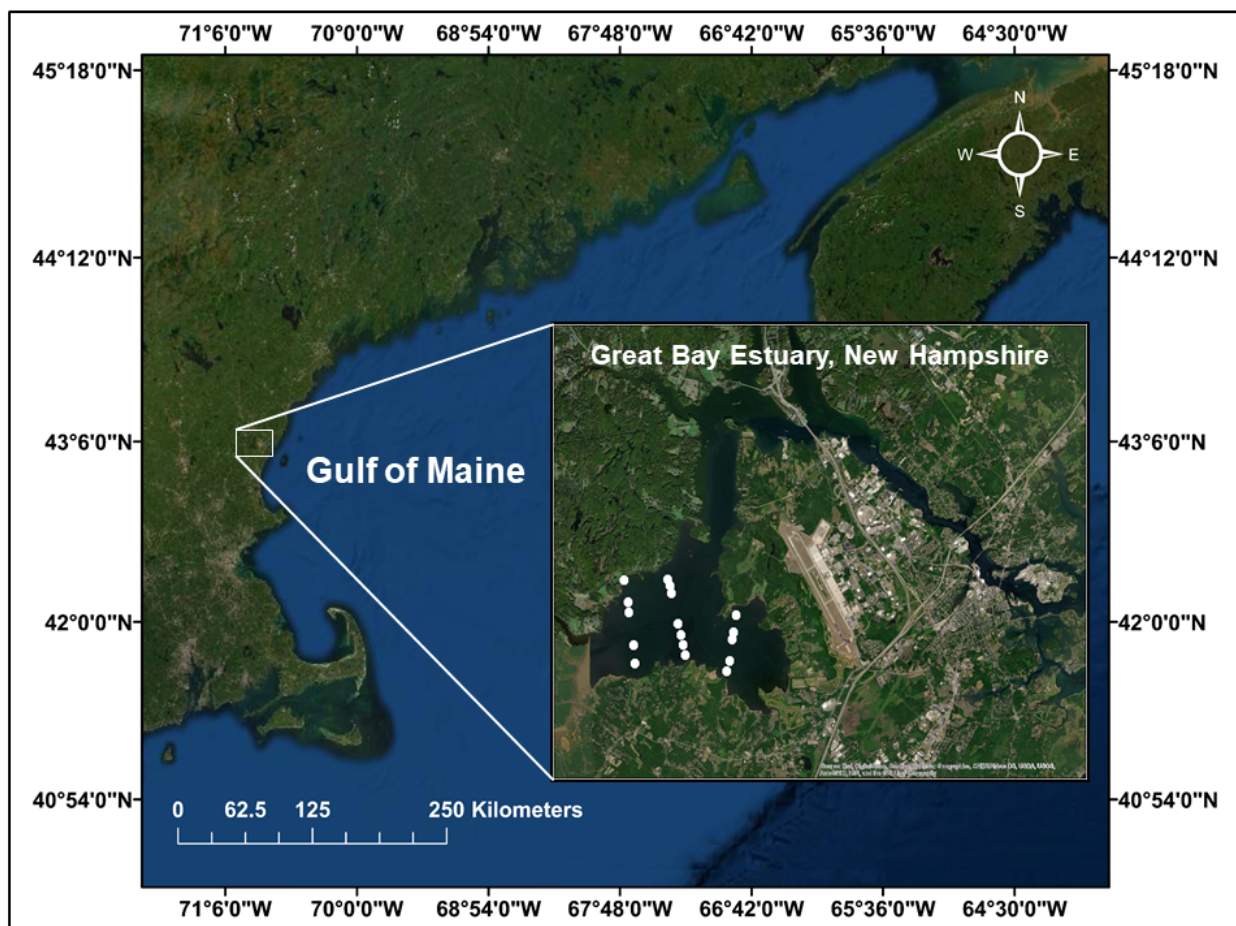
Figure 1. Map of Great Bay Estuary in New Hampshire, USA showing the locations of previously archived sediment cores obtained in 2015-2016 (white dots).
Note to Editors: this figure will require color printing, **2-column fitting image**

Sediment cores were obtained in GBE by scuba divers along 4 cross-estuary transects in 2015-2016 (Lucking et al. 2017). Cylindrical core sleeves (10.8 cm diameter) were inserted the seabed up to 30 cm depth and carefully extracted to minimize distortion of the upper and lower core sections. The cores were sectioned into 2 cm (+/- 1 mm) thick layers (corresponding to sediment volume of 183.22 cm^3 with 5% error) by forcing the mud upward with a levered press and slicing the extruded material into a clean sampling bag. Wet samples were stored at 4°C in a climate controlled refrigerated room. The subsections were oven-dried at 60-100°C for at least 24 hrs, cooled to room temperature in a desiccator, and stored dry in sealed containers.

We examined a total of 25 2-cm subsections across 17 cores (Fig. 1) for MP concentration. Morphology and sediment samples from the three deepest cores (0-30 cm) were subjected to radiometric depositional age determination. Age by depth in sediment cores was accomplished by radiometric dating performed by Flett Research, Ltd. with ^{210}Pb and ^{226}Ra, a method commonly used to obtain age by depth of sediments (Benninger, 1978; Farmer, 1978). The accumulation of sediment was determined using a procedure modified from Eakins and Morrison (1978) by measurement of the ^{210}Po granddaughter of ^{210}Pb, both of which are in secular equilibrium within 2 years of ^{210}Pb deposition (assuming a constant input of ^{210}Pb from the atmosphere). Sediment isotope accumulation rates were confirmed by ^{226}Ra determined by ^{222}Rn emanation using a procedure modified from Mathieu et al. (1988). Data were subjected to an iterative best fit slope regression model to determine the sediment accumulation rate, from which the age of each sediment section was estimated.

Selected upper, intermediate, and lower sections were subsampled for MP using a Sediment-Microplastic Isolation (SMI) unit via $ZnCl_2$ (1.45 g cm^{-3}) density separation to remove sediment and to isolate most MP from our samples (Hitchcock and Mitrovic 2019; Coppock et al. 2017). MPs in sediment cores were left to settle in the SMI unit for 12 hours before undergoing a vacuum filtration process onto 25 mm PTFE membrane filters (5.0µm, Sigma-Aldrich). Following the filtration process, samples were placed in a 1:1 mixture of KOH (30%) with NaClO (14%, Alfa Aesar) and held at 60°C for 24 h in a laboratory oven to digest biogenic matter (Lusher et al. 2016; Enders et al. 2016). Samples were then stained with Nile Red (10 µg mL^{-1}) and MP were visualized via confocal microscopy (Nikon A1R HD) (Erni-Cassola et al. 2017; Maes et al. 2017) to initially quantify putative MP. Visualization of MP via confocal microscopy were fluoresced in green (excitation: 480 nm; emission: 515 nm) under a 10x objective lens.

Because the visualization of MP by confocal microscopy cannot precisely identify the plastic type, elemental composition of MPs in selected sediment sections was assessed by infrared microscopy to provide an estimate of precision of our confocal determination. We washed particles from the original PTFE filters and for each platform, transferred to appropriate surfaces for viewing. For Fourier Transform Infrared microspectrometry (micro-FTIR) on both ThermoScientific Nicolet iN10MX and Shimadzu AIM9000 microscopes, we transferred MP to 47 mm 30µm stainless steel filters (Cellscreen, Chemglass Life Science). For analysis using Bruker Lumos II micro-FTIR, MP were transferred to 25mm 0.2µm AlOx filters (Whatman Anodisc). Finally, MP of four samples were transferred into a 70% EtOH slurry, applied to Kevley slides (Kevley Technologies, MIRRIR Low-e glass slides, NC0733469), and allowed to dry prior to analysis using Agilent 8700 LDIR. In each case, elemental compositions of MPs were determined using reference libraries and polymers were identified based on their spectrum compared to characteristic peaks. All four microscopes were capable of viewing and analyzing particles 10µm.

Noting that Nile Red co-stains biogenic material (rubber, chitin etc.) along with polymers (Erni-Cassola et al. 2017; Maes et al. 2017; Shim et al. 2016), samples sent for elemental composition analysis (micro-FTIR and LDIR) of MPs were used to validate and ensure that data obtained from staining methods were not overestimated. We note that plastic concentrations generated from this study should be construed as indicative rather than definitive, Additionally, we also employed various procedures to minimize laboratory contamination. Samples were always covered with aluminum foil caps and were

processed inside a fume hood when possible. Cotton lab coats and nitrile gloves were worn at all times when conducting laboratory procedures and all laboratory equipment was washed using filtered deionized water after use. Prior to and after use, all chemical solutions were vacuum filtered through a 0.2 μm filter to address potential laboratory contamination.

Statistical analyses, performed in R (v 3.6.3, R Core Team 2020), included tests for normality, and equal variance. Sediment sections were classified into the following categories: top, intermediate, and bottom sections of sampled cores. ANOVAs were performed to test for mean differences across depth sections and across the 3 transects (Fig 1). Quantitative data including MP quantity, density, type g-1 dry weight of sediment, were used in subsequent models and statistical determinations.

Microplastic type and density g^{-1} dry weight of sediment were used in numerical modeling experiments to estimate spatial distributions of MP concentrations in surficial seafloor sediments, and to assess the sensitivity of particle settling and bed erosion parameters to the spatial distribution of particles throughout the GBE. Concentrations of suspended particles, c_1, and settled particles, c_2, as a function of space and time were modeled with a simple coupled advection scheme given by

$$\frac{\partial c_1}{\partial t} + \vec{u}\nabla c_1 = -k_{st}(1-\theta)c_1 + k_{rs}\theta\sigma c_2 \tag{1}$$

$$\frac{\partial c_2}{\partial t} = k_{st}(1-\theta)c_1 - k_{rs}\theta\sigma c_2 \tag{2}$$

where $\vec{u}$ is the spatially and temporally varying depth-averaged velocity vectors, k_{st} is the setting rate, k_{rs} is the resuspension (or erodibility) rate, and t is time. The parameter θ is a binary function dependent on the spatial and temporally varying the fluid shear stress at the seabed, τ, relative to a critical value for resuspension, τ_{crit}, and given by

$$\theta(\boldsymbol{x},t) = \begin{cases} 1 & \tau \geq \tau_{crit} \\ 0 & \tau < \tau_{crit} \end{cases} \tag{3}$$

where **x** defines the 2-dimensional location within the model grid, and τ_{crit} is specified as 0.35 N m^{-2} following Eromes chamber experiments conducted on GBE cores by Percuoco et al. 2015 and Wengrove et al. 2015. The effects of sediment trapping by aquatic vegetation (e.g., eelgrass meadows) is also represented by binary function, σ, that suppresses the resuspension of settled particles within the meadows, and given by

$$\sigma(\boldsymbol{y}) = \begin{cases} 1 & no\ aquatic\ vegetation \\ 0 & within\ eelgrass\ meadows \end{cases} \tag{4}$$

where **y** defines the regions of the eelgrass meadows. The elimination of resuspension events within the eelgrass meadows is based on the assumption that bed stresses are greatly reduced within the canopy of the vegetation, effectively trapping the sediments (e.g., Beudin et al. 2017).

Two sets of simulations were conducted using velocity fields, $\vec{u}$, and bed shear stresses, τ, spanning the GBE estimated by Cook et al. (2019) using the Regional Ocean Modeling System (ROMS; Shchepetkin and McWilliams 2005; Haidvogel et al., 2008) coupled (after Choi et al. 2018) with equations 1-4 that predicts the spatial and temporal concentration of particles in the water column and settling of MP on the seafloor. Initial 5-day model simulations were initiated with a circular mound of unconsolidated MP located on the seafloor within the center of GBE (Fig. 3, upper left panel). MP properties included particle sizes (~0.02-0.6 mm) and density (~1.06 g cm^{-3}) and Stokes terminal fall velocity (based on seawater density of 1.027 g cm^{-3} and dynamic viscosity of 0.00141 Pa s at 10°C). Concentration settling rate, k_{st}, is given by the Stokes terminal velocity normalized by the total water depth (typically 1-5 m), and ranges ~0.005-4.5 day^{-1} for the range MP diameters. The model assumes

sediments to be suspended uniformly into the water column when flow velocities produce bed shear stresses that exceed the above defined τ_{crit} threshold. The resuspension parameter, k_{rs}, is not well constrained and assumed herein to have values that range the same order of magnitude as the settling rate. Simulations are performed across a range of values to examine the dependence of settled MP particle distributions across GBE on settling and resuspension rates. Suspended particles were dispersed horizontally by advection processes (equations 1 and 2). Particles settle out based on settling rates and where bed shear stresses are weak, and then potentially re-suspend again on the next ebb or flood tidal cycle. Subsequent simulations evaluated how MP might be deposited in GBE both with and without the presence of aquatic vegetation (eelgrass meadows) that change the properties of the bed shear stress (as in Cook et al. 2021). Observations of eelgrass meadows used for this study were taken from Short (2017; Fig 3, upper left panel) and simulations of particle flow were parameterized by the bed erodibility functions given by equations 3 and 4. Simulations also were conducted that assessed the sensitivity of deposited MP distributions to particle settling and resuspension parameters, k_{st} and k_{rs}, that grossly represent basic physical processes of settling and resuspension.

Sediment age determined by radiometric dating was found to increase in a linear fashion with depth. Accumulation rate was quite similar between two of the three cores aged; for those two cores, the top 6 cm of sediment indicated accumulation occurred over the past 10 years; the other dated core contained sediments that were aged >50 years at that depth. Numbers of particles detected by all three methods (Nile Red staining, micro-FTIR, and LDIR) were within an order of magnitude of one another and MP (and fragments of other materials, most notably rubber but also chitin and plant fibers that escaped biodegradation; Fig. 2C) were found in most sediment subsamples aged ≤ 50 years. Despite the detection of some biogenic particles, we do not believe MP concentrations found in this study are overestimated, given our results were within an order of magnitude. Furthermore, previous literature has attested the effectiveness of MP identification via Nile Red staining (Erni-Cassola et al. 2017; Maes et al. 2017; Shim et al. 2016). Thus, we reassert that our results are only indicative of MP concentrations present in the bay.

Across the 25 sediment sections analyzed, the range of MP detected was 0–675 MP g^{-1} sediment dry weight, with a median occurrence of 60 MP g^{-1}, and a mean of 116 ± 21 MP g^{-1}. All results reported hereafter are presented as mean ± standard error of the mean. Microplastics were more abundant in intermediate-aged sediments (171±65 MP) than they were in older (42±7) and newly deposited (118±25) sediment sections, albeit not to a significant degree ($p=0.26$). Additionally, there were no significant differences detected in the number of particles detected across transects ($p=0.17$). Morphology of MP was variable and differed significantly across cores in terms of length ($p<0.001$). Particle lengths were 53 ± 0.5 µm and ranged from 5- 1785 µm. Sections analyzed for elemental composition contained a mixture of polymers. Polymers found in the first 0-2 cm sediment sections were dominated by the presence of polyurethane (PU, ~22%), followed by polyvinylchloride (PVC, ~8%), polyvinyl alcohol (PVA, ~7%), and polyamide (PA, ~6%). Plastic types in the 0-2 cm sections were variable with a total of 25 different plastic types detected whereas polymers detected in the 2-4 cm sediment sections had fewer different MP types (12), predominantly polyvinylchloride (PVC, ~30%) or polypropylene (PP, ~27%). Finally, sediments analyzed in the 4-6 cm sections had a total of 23 different polymers, the most abundant being ~13% PU, ~7% PA, and ~6% polyethylene terephthalate (PET).

The numerical simulations indicated that unconsolidated MP initially on the seafloor within the center of GBE were suspended rapidly by the tidal flows and advected and deposited over just a few tidal cycles in regions of low bed shear stress near the fringes of the GBE, especially in the absence of aquatic vegetation (Fig. 3, lower right panel). In the presence of eelgrass, particles also were efficiently trapped by the reduced erodibility and shear stresses within the meadows (Fig 3, lower left panel), consistent with the notion that eelgrass meadows act as effective sinks for suspended MP. Much higher concentrations of particles remained in – or were brought back into – suspension during model runs without vegetation compared with model runs that included eelgrass meadows, indicating higher numbers of MP that disperse widely and may leave GBE in the absence of aquatic vegetation. The ensemble of all model

simulations including eelgrass meadows showed that erosion rate (easily eroded versus erosion-resistant conditions) was the most important determinant of MP spatial distribution in GBE. Simulations showed that resuspended particles were repeatedly suspended, advected, deposited, and resuspended by the tidally varying flow until the MP permanently settled out in regions of low bed shear stress (i.e., weak erodibility conditions with low erosion rate) associated with the eelgrass meadows or fringes of the Bay. Far fewer MP remained in suspension during vegetated model runs compared with the non-vegetated model indicating a much higher number of particles ultimately remain within the GBE under realistic conditions. Under conditions of weak settling velocity (i.e., more buoyant particles), fewer MP will settle to the bottom, a situation that increases the likelihood that more MP in the water column will be flushed from GBE. Interestingly, the ensemble of all model simulations (Fig. 3, upper right panel) indicated a higher dependence on bed-erodibility, k_{rs}, than on settling rate, k_{st}. The latter term is determined by MP density and size and is complicated by poorly understood flocculation processes that increase sinking rates, whereas k_{rs} is strongly determined by characteristics of the seafloor that may include the presence or absence of aquatic vegetation. Collectively, these results indicate that bed characteristics are likely a more controlling factor in MP distribution than the particle properties themselves.
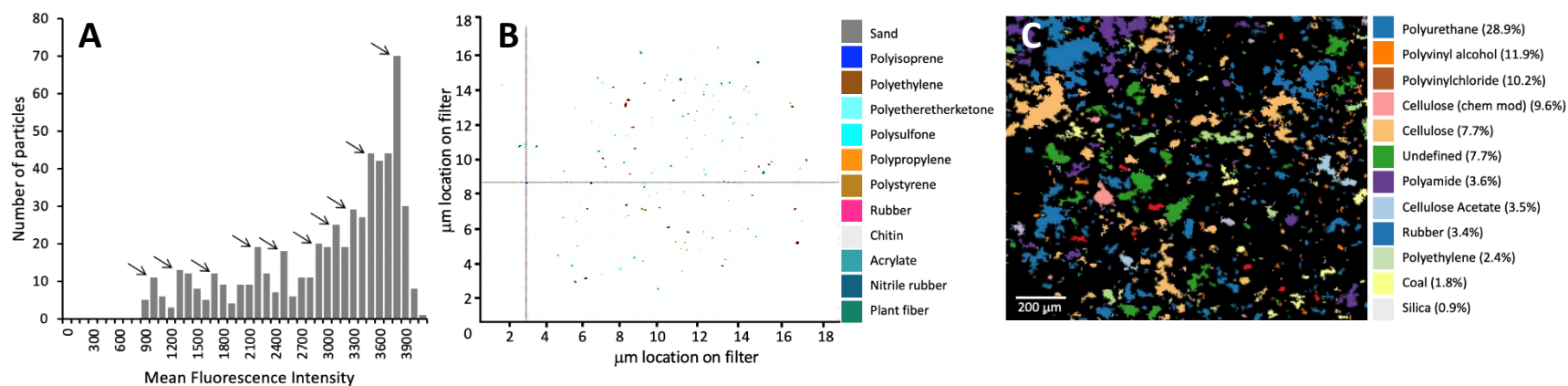
Figure 2. Three renditions of occurrence and morphology of microplastic particles found in representative sediment cores from Great Bay Estuary. A: Multiple fluorescence peaks (arrows) of Nile Red stained, confocal imaged MP from a sediment core section signify relative abundance of putatively different types of plastic particles. B: Particle map generated by micro-FTIR for a small section (300 μm^2) of an AlOx filter shows multiple (false colored) plastic particles isolated from a sediment sample but also biogenic substances that escaped digestion. C: Partial view of LDIR particle map from a sediment sample shows multiple plastics and also biogenic substances (false color key sorted by frequency out of 3,283 particles).

Note to Editors: this figure will require color printing, 2-column fitting image
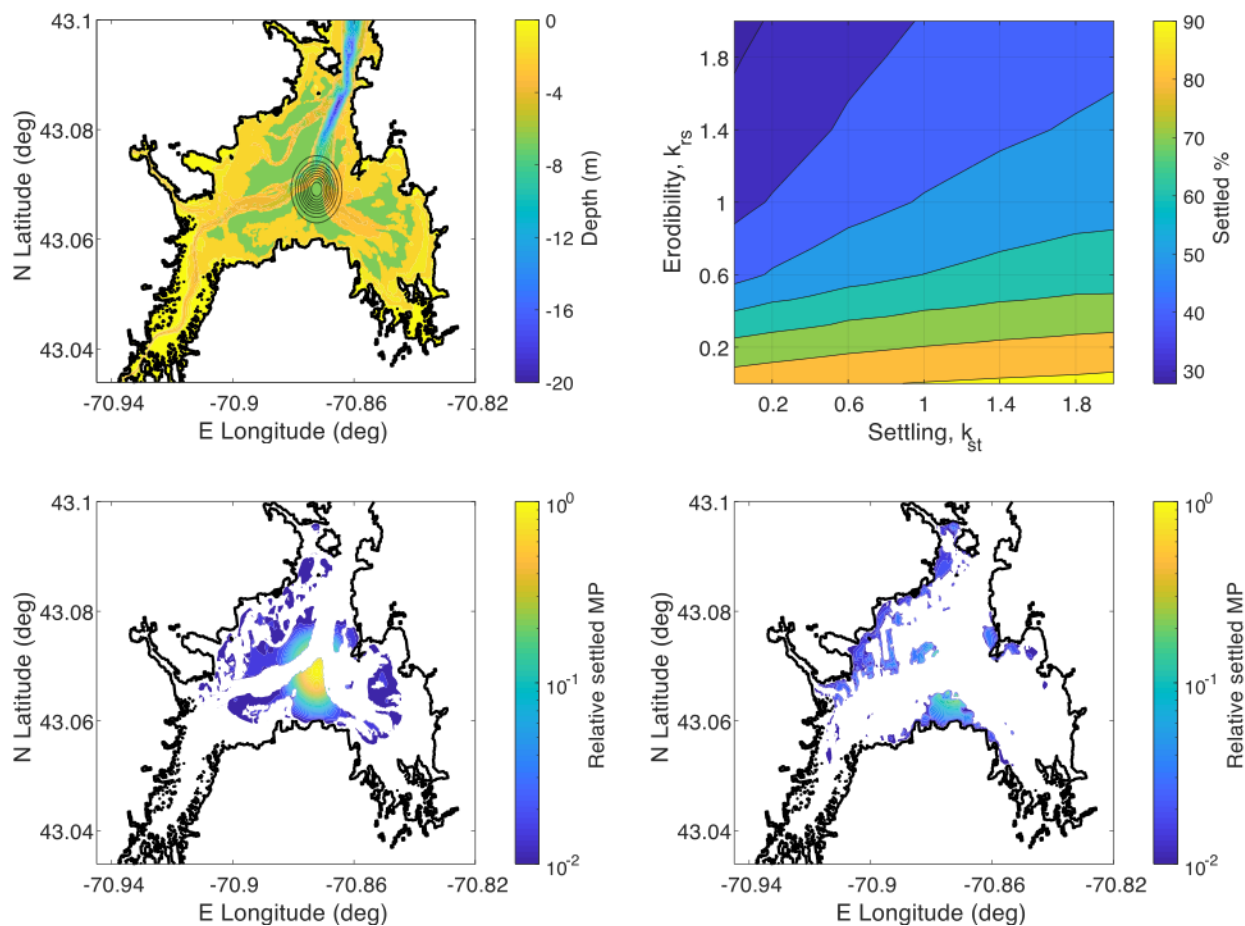
Figure 3. Spatial distribution of MP particles after 5-day model simulations. Upper Left: Bathymetry of the GBE (color contours relative to NAVD88, approximately mean sea level) and the spatial distribution of eelgrass meadows (green areas) from 2016. Also shown are contours of the initial particle distribution on the seabed in the center of the estuary. Lower Left: Single simulation result in the presence of eelgrass showing that MP are effectively trapped within eelgrass meadows. Lower Right: Single simulation result in the absence of eelgrass meadows showing that MP are transported to the sides of GBE where they settle in areas along the fringes and shallow areas of the Bay (areas with low hydrodynamic velocities, low erodibility, and weak bed shear stress). Upper Right: Ensemble of all simulations showing contours of % MP deposited on the seafloor as a function of bed-erodibility, k_{rs}, and settling rates, k_{st}. Results show that bed-erodibility is a stronger determinant of MP concentration in the sediments than settling properties.

Note to Editors: this figure will require color printing, **2-column fitting image**

There is a pressing need to determine the sources, distribution, and fate of MP particles so that interactions of MP with aquatic organisms that are harvested for human consumption can be understood. Deepening our knowledge of MP in estuarine systems is a necessary component of addressing the knowledge gap of the realistic levels of risk these particles pose to living resource populations (Lenz et al. 2016). To our knowledge, this is the first study to generate temporal and spatial patterns of MPs using preserved cores, thus providing a baseline for the historical complement of MP in an estuarine system. Our present study indicates that concentrations of MPs have likely changed over time, with greatest MP concentrations at intermediate aged sediments. Potential declines observed in relative MP abundance at

newly deposited sediments could potentially be attributed to improved filter systems at upgraded and newly constructed water treatment facilities. Future studies would benefit from monitoring of MPs at water treatment facilities to understand the effectiveness of newly implemented filtration systems.

We conclude that variations in spatial MP concentrations are likely affected by the presence of aquatic vegetation (eelgrass meadows) where plant structure will trap or slow the transport of particles within estuaries that contain eelgrass, reducing erodibility and bed shear stress and promoting settling in those areas. Our findings are consistent with recent studies demonstrating the potential for eelgrass meadows to be a trap and sink for MP (de los Santos et al. 2021; Huang et al. 2020). Although eelgrass meadows in the GBE are on the decline, recent assessments indicate that meadows continue to cover a large area of the estuary (600 hectares; ~15% of the GBE) (Barker 2020). Consequently, the occurrence and concentrations of MPs in the GBE could be augmented in the presence of the high coverage of eelgrass meadows. Furthermore, increased concentrations of MP at eelgrass meadows are likely to have negative implications on biota that reside in these meadows, namely through higher ingestion rates of MP particles. The potential accumulation of MPs on eelgrass meadows are a cause for concern, given the use and dependency of these areas by many commercial species (Heck et al. 1995), and the potential for plastics to transfer up towards higher trophic levels. Although this study is primarily focused on eelgrass meadows, our findings could potentially translate to other vegetated structures such as macroalgae. Feng et al (2020) suggested four mechanisms (twining, embedment, wrapping, and attachment) facilitating the trapping of MP on *Ulva prolifera;* a macroalga. Findings from Feng et al (2020) are important to note because researchers in GBE have observed an increased prevalence of nuisance macroalgae (*Gracilaria tikvahiae* and *Ulva lactuca)* in recent years (Nettleton et al. 2011), which are also likely contributing to the declines in eelgrass meadows (Short 2012). Given the growing presence of macroalgae in the GBE and their ability to trap MP (Feng et al. 2020), it is imperative that we better understand how accumulation rates of MPs onto sediments differ in macroalgal structures relative to other vegetated structures.

Our study established a rough baseline of ambient MP levels, types, and accumulation. Findings from this study provide current and historical context on the extent of MP pollution in the GBE, and will help advance future research efforts in the area. The coupled hydrodynamic and particle tracking model provided a mechanism for predicting MP spatial distribution patterns, understanding the behavior of MP settling, and tracing the evolution of MP concentrations in sediments. Future studies coupling MP concentration and identity found in both water and sediments will facilitate creation of illustrative models that more adequately describe the present potential for introduction, movement, and distribution of MP in estuaries. Verified model visualizations will promote data usage by harvesters, farmers, and resource managers enabling new strategies to cope with the presence of MPs, modify harvesting procedures, and hot-spot avoidance for future restoration activities.

References
Arthur C, J Baker, H Bamford. 2009. Proceedings of the International Research Workshop on the
     Occurrence, Effects, and Fate of Microplastic Marine Debris. Group: 530.

Barker, Seth, "Eelgrass Distribution in the Great Bay Estuary and Piscataqua River for 2019: Final Project Report submitted to the Piscataqua Region Estuaries Partnership" (2020). PREP Reports & Publications. 438.

Benninger LK. 1978. Pb-210 balance in Long Island Sound. *Geochimica and Cosmochimica Acta* 42:1165-1174.

Beudin, A, Kalra TS, Ganju NK, Warner JC. 2017. Development of a coupled wave-flow-vegetation interaction model. *Comput. Geosci.*, 100:76-86.

Choi, JG, Jo YH, Moon IJ, Park J, Kim DW, Lippmann TC. 2018. Physical forces determine the annual bloom intensity of the giant jellyfish *Nemopilema nomurai* off the coast of Korea, *Reg. Studies in Mar. Sci.*, 24, 55-65.

Cook SE, Lippmann TC, Irish JD. 2019. Modeling nonlinear tidal evolution in an energetic estuary. *Ocean Modelling* 136:13-27.

Cook, SE, Lippmann TC, Koetje K, Wengrove M, Foster D. 2021. The influence of submerged aquatic vegetation on modeled estimates of bed shear stress and nutrient resuspension in a tidally dominant estuary, *Estuarine, Coastal, and Shelf Science*, *sub judice*.

Eakins, JD, Morrison RT. 1978. A new procedure for the determination of lead-210 in lake and marine sediments. *International Journal of Applied Radiation and Isotopes*. 29: 531-536.

Estahbanati, S. Fahrenfeld N. L. 2016. Influence of wastewater treatment plant discharges on microplastic concentration in surface water. *Chemosphere* 162:277-284.

Farmer JG. 1978. The determination of sedimentation rates in Lake Ontario using the Pb-210 dating method. *Canadian Journal of Earth Sciences* 15:431-437.

Feng Z, Zhang T, Shi H, Gao K, Huang W, Xu J, Wang J, Wang R, Li J, Gao G. 2020. Microplastics in bloom-forming macroalgae: Distribution, characteristics and impacts. *Journal of Hazardous Materials* 397: 122752.

Granek EF, Brander SM, Holland EB. 2020. Microplastics in aquatic organisms: Improving understanding and identifying research directions for the next decade. *Limnology and Oceanography Letters* 5: 1–4.

Haidvogel DB, H Arango, WP Budgell, BD Cornuelle, E Curchitser, E Di Lorenzo, K Fennel, WR Geyer, AJ Hermann, L Lanerolle, J Levin, JC McWilliams, AJ Miller, AM Moore, TM Powell, AFShchepetkin, CR Sherwood, RP Signell, JC Warner, J Wilkin. 2008. Ocean forecasting in terrain-following coordinates: formulation and skill assessment of the Regional Ocean Modeling System, *Journal of Computational Physics* 227:3595–3624.

Heck KL, Able KW, Roman CT, Fahay MP. 1995. Composition, Abundance, Biomass, and Production of Macrofauna in a New England Estuary: Comparisons among Eelgrass Meadows and Other Nursery Habitats. Estuaries 18: 379.

Huang Y, Xiao X, Xu C, Perianen YD, Hu J, Holmer M. 2020. Seagrass beds acting as a trap of microplastics - Emerging hotspot in the coastal region? Environmental Pollution 257: 113450.

Kaiser D, Kowalski N, Waniek JJ. 2017. Effects of biofouling on the sinking behavior of microplastics. *Environmental Research Letters* 12:124003.

Law KL. 2017. Plastics in the marine environment. *Annual Review of Marine Science* 9:205-229.Lenz R, K Enders, TG Nielsen. 2016. Microplastic exposure studies should be environmentally realistic. *Proceedings of the National Academy of Sciences* 113:E4121-E4122.

Lucking G, Stark N, Lippmann TC, Smyth S. 2017. Variability of in situ sediment strength and pore pressure behavior of tidal estuary surface sediments. *Geo-Marine Letters* 37: 441–456.

Lusher AL, Welden NA, Sobral P, Cole M. 2017. Sampling, isolating and identifying microplastics ingested by fish and invertebrates. Analytical Methods 9: 1346–1360.

Maes T, Jessop R, Wellner N, Haupt K, Mayes AG. 2017. A rapid-screening approach to detect and quantify microplastics based on fluorescent tagging with Nile Red. *Scientific Reports* 7: 44501.

Mason SA, Garneau D, Sutton R, Chu Y, Ehmann K, Barnes J, Fink P, Papazissimos D, Rogers D. 2016. Microplastic pollution is widely detected in US municipal wastewater treatment plant effluent. *Environmental Pollution* 218:1045-1054.

Mathalon A, Hill P. 2014. Microplastic fibers in the intertidal ecosystem surrounding Halifax Harbor, Nova Scotia. *Marine Pollution Bulletin* 81: 69–79.

Mathieu, GG, Biscaye PE, Lupton RA, Hammond DE. 1988. System for measurement of 222Rn at low levels in natural waters. *Health Physics* 55:989-992.

Murphy F, Ewan C, Carbonnier F, Quinn B. 2016. Wastewater treatment works (WwTW) as a source of microplastics in the aquatic environment. *Environmental Science & Technology* 50:5800-5808.

Murray F, Cowie PR. 2011. Plastic contamination in the decapod crustacean Nephrops norvegicus (Linnaeus, 1758). *Marine Pollution Bulletin* 62: 1207–1217.

Nettleton, JC, Neefus, CD, Mathieson, AC, and Harris, LG. 2011.Tracking environmental trends in the Great Bay Estuarine System through comparisons of historical and present-day green and red algal community structure and nutrient content. PREP Reports & Publications. 374. https://scholars.unh.edu/prep/374

Percuoco VP, Kalnejais LH, Officer LV. 2015. Nutrient release from sediments of the Great Bay Estuary, N.H. USA. *Estuarine Coast. Shelf Sci.*, 161:76-87.

R Core Team (2020). R: A language and environment for statistical computing. R Foundation for Statistical Computing, Vienna, Austria. URL https://www.R-project.org/.

Rocha-Santos T, Duarte AC. 2015. A critical overview of the analytical approaches to the occurrence, the fate and the behavior of microplastics in the environment. *Trends in Analytical Chemistry* 65:47-53.

de los Santos CB, Krång AS, Infantes E. 2021. Microplastic retention by marine vegetated canopies: Simulations with seagrass meadows in a hydraulic flume. Environmental Pollution 269: 116050.

Shchepetkin AF, McWilliams JC. 2005. The Regional Oceanic Modeling System (ROMS): A split-explicit, free-surface, topography-following-coordinate oceanic model, *Ocean Modeling* 9 ;347–404.

Shim WJ, Song YK, Hong SH, Jang M. 2016. Identification and quantification of microplastics using Nile Red staining. Marine Pollution Bulletin 113: 469–476.

Short FT. 1992. The ecology of the Great Bay Estuary, New Hampshire and Maine: An estuarine profile and bibliography. Page 222. Coastal Ocean Program Publ.

Short, FT. 2012. "Eelgrass Distribution in the Great Bay Estuary for 2010" (2012). PREP Reports & Publications. 4. https://scholars.unh.edu/prep/4

Short, FT. 2017. SeagrassNet Monitoring in Great Bay, New Hampshire, 2016. PREP Reports & Publications. 392. https://scholars.unh.edu/prep/392.

Sussarellu R, Suquet M, Thomas Y, Lambert C, Fabioux C, Pernet MEJ, Le Goïc N, Quillien V, Mingant C, Epelboin Y, Corporeau C, Guyomarch J, Robbens J, Paul-Pont I, Soudant P, Huvet A. 2016. Oyster reproduction is affected by exposure to polystyrene microplastics. Proceedings of the National Academy of Sciences 113: 2430–2435.

vanCauwenberghe L, Devriese L, Galgani F, Robbens J, Janssen CR. 2015. Microplastics in sediments: a review of techniques, occurrence, and effects. *Marine Environment Research*. 111:5-17.

Trowbridge P. 2007. Hydrological Parameters for New Hampshire's Estuaries. PREP Reports & Publications. 130.https://scholars.unh.edu/prep/130

Wengrove, ME, Foster DL, Kalnejais LH, Purcuoco V, Lippmann TC. 2015. Field and laboratory observations of bed stress and associated nutrient release in a tidal estuary, *Estuarine, Coastal, and Shelf Science*, 161, 11-24.

Zhang X, Chen J, Li J. 2020. The removal of microplastics in the wastewater treatment process and their potential impact on anaerobic digestion due to pollutants association. *Chemosphere* 251: 126360.